

# Influence of Branching on Network Formation and the Thermomechanical Properties of UV-Curable Polyester Powder Coating Resins

Theodore J. Hammer, Coleen Pugh, and Mark D. Soucek\*



Cite This: *Ind. Eng. Chem. Res.* 2022, 61, 11444–11454



Read Online

ACCESS |



Metrics & More



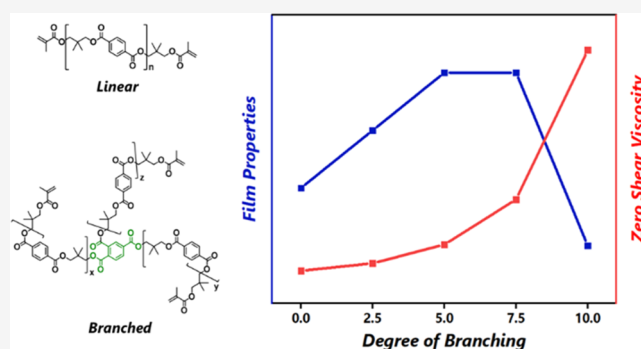
Article Recommendations



Supporting Information

**ABSTRACT:** A series of branched, UV-curable polyester oligomers were synthesized from neopentyl glycol, terephthalic acid, and variable amounts of trimellitic anhydride (TMA).  $^1\text{H}$  NMR spectroscopy and MALDI-ToF-MS confirmed that TMA was successfully incorporated into the oligomeric backbone. Differential scanning calorimetry experiments and zero-shear viscosity measurements were conducted to probe the thermal and rheological properties of the branched polyester resins. The  $T_g$  and the zero-shear melt viscosity were affected by the extent of branching as well as the functionality of the end group. UV-cured thin films were subsequently prepared and characterized via differential scanning calorimetry, thermal gravimetric analysis, dynamic mechanical analysis, tensile tests, and Soxhlet extractions.

In general, the crosslink density of the films increased with the extent of branching. Linear and lightly branched samples (i.e., 2.5 and 5.0 mol % TMA) had higher % elongations at break, while the more highly branched samples (i.e., 7.5 mol % TMA) had higher Young's moduli and tensile strengths. However, further increases in the extent of branching (i.e., 10.0 mol % TMA) negatively affected the mechanical properties of the film due to poor crosslinked network development. The insights from this study highlight the importance of optimizing the extent of branching for UV-curable polyester coating resins.



## INTRODUCTION

Thermoset powder coatings are a class of high-performance coatings that provide excellent mechanical properties, good weatherability, and high durability.<sup>1</sup> Powder coatings differ from traditional liquid coating systems in that they are handled, manipulated, and applied as dry powders. Because powder coatings are free of organic solvents, they are inherently less toxic and more environmentally friendly than many other coating technologies. Despite the many advantages that are associated with thermoset powder coatings, there are several disadvantages as well. One of the biggest drawbacks with thermally cured powder coatings is the harsh curing conditions. Curing temperatures of 180–200 °C for 10–15 min is common. This effectively limits the application potential of most thermoset powder coatings to metal substrates. Another drawback with thermally cured powder coatings is the competition that takes place between crosslinking and film formation. Because these two processes occur concomitantly, there is an increased possibility that film defects will occur.

To circumvent these drawbacks, UV-curable powder coatings were introduced.<sup>2</sup> UV-curable powder coatings offer many of the same advantages as traditional powder coatings, with the added benefits of lower curing temperatures and the ability to separate the film formation and curing processes.<sup>3</sup> Most UV-

curable powder coating resins are based on either methacrylated polyesters or acrylated epoxies.<sup>4</sup> UV-curable polyester resins are generally prepared using a two-step one-pot process wherein a carboxylic acid-terminated polyester is prepared first and is then subsequently reacted with glycidyl methacrylate to yield a methacrylate-terminated resin.<sup>5,6</sup> Twigt and Van der Linde prepared a crystalline unsaturated polyester based on 1,6-hexanediol, fumaric acid, and terephthalic acid and crosslinked it with a divinyl ether molecule.<sup>7</sup> The crosslinked films demonstrated excellent hardness, adhesion, and sandability. Moens et al. prepared UV-curable powder coating formulations from blends of amorphous and semi-crystalline resins.<sup>5</sup> The powder coating formulations had excellent storage stability, film formation properties, and impact resistance.

Changing the macromolecular architecture of a polymeric material is an approach that can be used to alter the rheological, thermal, and mechanical properties of a

**Received:** March 1, 2022

**Revised:** July 1, 2022

**Accepted:** July 11, 2022

**Published:** July 27, 2022



polymer.<sup>8–10</sup> Some of the different types of polymer architectures that have been prepared include graft copolymers (e.g., combs and brushes),<sup>11</sup> block copolymers,<sup>12,13</sup> telechelic polymers,<sup>14–16</sup> branched and hyperbranched polymers,<sup>17–21</sup> and dendrimers.<sup>22–25</sup> Branched and hyperbranched polymers are of particular interest for various commercial applications. A common approach that is used to change the architecture of a step-growth polymer is to incorporate polyfunctional monomers (i.e., a monomer with a functionality that is  $\geq 3$ ) into the polymer backbone. In the field of coatings, for example, polyfunctional monomers such as trimethylolpropane (TMP) are incorporated into polyester resins to increase the crosslink density of the film.<sup>26</sup>

Most powder coating resins contain a small amount (usually 2–3 mol %) of trifunctional monomer to impart branching.<sup>1,26,27</sup> This modification reduces crystallinity and improves the thermomechanical properties of the coating. Hyperbranched and dendritic UV-curable powder coating resins have also been reported. Johansson et al. synthesized crystalline dendrimers by grafting long polycaprolactone chains onto a polyfunctional core molecule, Bolthorn H<sub>2</sub>O.<sup>28</sup> The terminal hydroxyl groups of the polycaprolactone segments were subsequently functionalized with methacrylate groups to yield UV-curable resins. The crosslinked films were hard and scratch-resistant. Follow-up studies by the same group explored how structural variations of the dendrimer changed its melt viscosity before and during the UV-curing process.<sup>29,30</sup> Wei et al. also prepared UV-curable dendritic polyether-amide oligomers that had  $T_g$ s up to 43 °C and  $T_m$ s around 122–123 °C.<sup>31</sup> Crosslinked thin films had pendulum hardnesses up to 340 s. Cheng et al. prepared UV-curable hyperbranched polyester–amide oligomers from tris-(hydroxymethyl)-aminomethane and succinic anhydride.<sup>32</sup> The hydroxyl-terminated scaffold was subsequently functionalized with an isophorone diisocyanate-2-hydroxyethyl acrylate adduct to introduce UV-curable groups. Photo-DSC studies identified conversions up to 70% and pendulum hardness measurements that approached 300 s.

Although several investigations have explored the use of hyperbranched and dendritic powder coating resins, there have been no systematic studies focusing on the extent of branching in conventional systems, i.e., those that are principally derived from typical polyester powder coating monomers such as neopentyl glycol (NPG) and terephthalic acid (TPA). In this study, a series of branched, UV-curable polyester oligomers were synthesized from NPG, TPA, and variable amounts of trimellitic anhydride (TMA). The extent of branching was controlled by changing the feed ratio of TMA. The influence that branching had on the rheological and thermal properties of the different end-functionalized oligomers was evaluated. UV-curable formulations were subsequently prepared, and the thermal, viscoelastic, and mechanical properties of the crosslinked films were studied.

## EXPERIMENTAL SECTION

**Materials.** All reagents and solvents were used as received without further purification unless otherwise noted. Acetic anhydride ( $\geq 99\%$ ), benzoin (98%), 4-dimethylaminopyridine (DMAP; 99%), dibutyltin (IV) oxide (DBTO;  $>98\%$ ), hydroquinone (99%), methacrylic anhydride (MAAn; 94%), terephthalic acid (TPA; 98%), trimellitic anhydride (TMA; 97%), and triethylamine (TEA; 99%) were obtained from Sigma-Aldrich. Neopentyl glycol (NPG; 99%) was obtained

from Alfa Aesar. Dichloromethane (DCM; 99.9%), ethanol (reagent grade), methanol (MeOH;  $\geq 99.8\%$ ), and tetrahydrofuran (THF;  $>99\%$ ) were obtained from Fisher Scientific. Irgacure 2959 2-Hydroxy-4'-(2-hydroxyethoxy)-2-methylpropiophenone and Irgacure 819 (phenylbis(2,4,6-trimethylbenzoyl)phosphine oxide) were obtained from BASF. MODAFLOW 6000 was kindly supplied by Allnex. DMAP was recrystallized from ethyl acetate prior to use. Steel Q-panels (AQ-36) were obtained from Q-lab Corporation (Cleveland, OH).

**Techniques and Instrumentation.** All reactions were conducted under an atmosphere of N<sub>2</sub> using standard Schlenk line techniques unless otherwise noted. All <sup>1</sup>H (300 MHz) NMR spectra ( $\delta$ , ppm) were recorded on a Varian Mercury 300 MHz NMR spectrometer using CDCl<sub>3</sub> as solvent. Number-average molecular weight ( $M_n$ ) and dispersity ( $\bar{D}$ ;  $\bar{D} = M_w/M_n$ ) were measured with an HLC-8320 SEC from Tosoh equipped with a refractive index detector. The samples were analyzed at 40 °C with Styragel HT2, HR1, HR0.5, and 500 Å Ultrastaygel columns and compared against a polystyrene (SEC<sub>PSt</sub>) standard. THF was used as the eluent at a flow rate of 1.0 mL/min. Samples were prepared at a concentration of 5.0 mg/mL and were filtered through a 0.45  $\mu$ m syringe filter prior to injection. MALDI-ToF-MS spectra were recorded on a Bruker Ultra-Flex III MALDI-ToF/ToF mass spectrometer (Bruker, Billerica, MA) equipped with a Nd:YAG laser emitting at 355 nm. The instrument was operated in positive ion mode. Samples were dissolved in THF to a final concentration of 10 mg/mL. *Trans*-2-[3-(4-*tert*-butylphenyl)-2-methyl-2-propenylidene]malononitrile (DCTB) (20 mg/mL) served as the matrix, and sodium trifluoroacetate (NaTFA) (10 mg/mL) served as the cationizing agent. The latter two were prepared and mixed in the ratio 1:10 (v/v), respectively. Matrix:salt and sample solutions were applied on the MALDI-ToF-MS target plate using a sandwich method. Bruker's flexAnalysis software was used for analysis.

Differential scanning calorimetry (DSC) experiments were performed on a TA Instruments model Q2000. The sample size was approximately 5.00 mg. Heat/cool/heat cycles were conducted using 20 °C heating and cooling rates. The glass-transition temperature ( $T_g$ ) was taken as the middle of the inflection point on the second heating cycle. All samples were run in duplicate. Thermogravimetric analysis (TGA) was conducted on a TA instruments model Q50 under an N<sub>2</sub> atmosphere. Samples were measured from ambient conditions to 600 °C with a heating rate of 10 °C/min. Dynamic mechanical analysis (DMA) was conducted on a TA instrument model Q800 in tensile mode. Samples were tested at 1 Hz frequency, 0.1% strain, and at a heating rate of 4 °C/min from 0 to 200 °C. All samples were run in triplicate. Tensile testing was carried out using procedures that were similar to ASTM D882. All tensile experiments were conducted on an Instron 5567 with a 1 kN load cell. Samples were run at a crosshead speed of 5 mm/min. A minimum of 4 replicates were conducted for each sample. Error was expressed as standard deviation. Free-standing films were obtained by solvent-casting (further details are provided below). Rectangular samples with the dimensions of approximately 25 × 6 × 0.20 mm<sup>3</sup> (length × width × thickness) were used for both DMA and tensile testing. Zero-shear rate viscosity measurements were conducted on a Discovery HR-2 (DHR-2) rheometer. Experiments were carried out at  $T_g + 50$  °C

using 25 mm parallel plate geometry. An angular frequency sweep ( $10^{-3}$ –100 rad/s) was conducted with a total of five points per decade. Gel content was determined from Soxhlet extractions. Experiments were conducted over the course of 24 h using THF as the solvent. Samples were subsequently dried for 24 h in an 80 °C vacuum oven prior to obtaining the final mass; initial sample weights were approximately 0.2 g. All Soxhlet extractions were performed in triplicate. Pencil hardness (ASTM D3363) and direct impact resistance (ASTM D2794) coatings tests were conducted on coated steel Q-panels.

**Synthesis of a Hydroxyl-Terminated Polyester Oligomer Containing 5 mol % TMA.** The following procedure describes a typical melt polycondensation reaction. This particular example was conducted with 5 mol % TMA; the other polyester oligomers were synthesized in the same manner, albeit with different amounts of TMA. NPG (66.90 g, 0.64 mol), TPA (78.80 g, 0.47 mol), TMA (4.79 g, 0.02 mol), and dibutyltin oxide (0.3026 g, 0.2 wt %) were added to a 500 mL, round-bottom flask equipped with an overhead mechanical stirrer, N<sub>2</sub> inlet, and a condenser fitted with a Dean-Stark trap. The round-bottom flask was placed into a mantle and heated to 185 °C, where it was held for 1 h, with stirring. The reaction temperature was then slowly raised, over the course of 5 h, to 250 °C, where it was held for another 4.5 h. By this point in the reaction, water was no longer regularly distilling (>95% of the theoretical water had been collected). The reaction temperature was reduced to 230 °C, and vacuum distillation was established for 1 h to remove any water or unreacted monomer and to drive the reaction to completion. The viscous melt was then immediately poured into a pan and left overnight to solidify. An optically clear and colorless, glassy solid was obtained. SEC<sub>PSt</sub>  $M_n = 3.23 \times 10^3$  Da,  $\bar{D} = 2.04$ ;  $T_g = 59$  °C; acid number = 3.33 mg KOH/g resin. <sup>1</sup>H NMR (Figure S1),  $\delta$  (ppm): 0.91–1.17 (–CH<sub>3</sub>), 3.40–3.51 (–CH<sub>2</sub>OH), 4.20–4.29 (–CO–O–CH<sub>2</sub>–), 7.72–7.75 (ArH), 8.06–8.08 (ArH), 8.38 (ArH).

**Synthesis of a Methacrylate-Terminated Polyester Containing 5 mol % TMA.** The following procedure describes the functionalization reaction of the 5 mol % TMA polyester using methacrylic anhydride. The other polyester oligomers were functionalized in the same manner. The aforementioned hydroxyl-terminated polyester (81.08 g, 0.04 mol), TEA (12.58 g, 0.12 mol), DMAP (0.4899 g, 0.004 mol), hydroquinone (0.1034 g, 0.94 mmol), and DCM (300 mL) were added to a 1 L round-bottom flask and magnetically stirred while cooling in an ice bath. Once homogeneous, methacrylic anhydride (19.13 g, 0.12 mol) in DCM (50 mL) was added dropwise to the reaction vessel. The ice bath was removed, and the reaction was left to continue stirring overnight. The clear and colorless solution was concentrated on a rotavap to approximately half its original volume and was then precipitated dropwise into 1 L of cold ethanol. A fine white precipitate was collected by filtration and was then washed with MeOH (150 mL, 3 $\times$ ). After drying in a room temperature vacuum oven for several days, a white powdery solid was obtained (80.73 g). SEC<sub>PSt</sub>  $M_n = 3.86 \times 10^3$  Da,  $\bar{D} = 1.91$  (post precipitation mass and dispersity);  $T_g = 49$  °C. <sup>1</sup>H NMR (Figure S2),  $\delta$  (ppm): 1.10–1.17 (–CH<sub>3</sub>), 1.94 (–CH<sub>3</sub>, methacrylate), 4.06 (–CO–O–CH<sub>2</sub>–, end-group adjacent), 4.18–4.29 (–CO–O–CH<sub>2</sub>–), 5.57 (C=CH<sub>2</sub>), 6.11 (C=CH<sub>2</sub>), 7.72–7.82 (ArH), 8.08 (ArH), 8.17–8.19 (ArH), 8.34–8.38 (ArH).

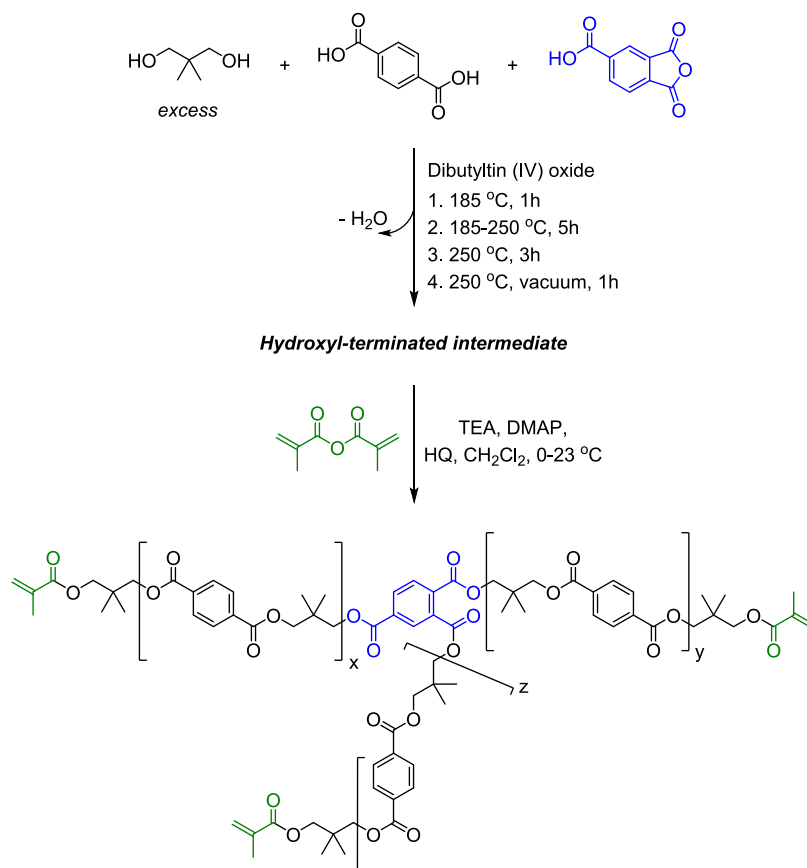
**Synthesis of an Acetyl-Terminated Polyester Containing 5 mol % TMA.** The following procedure describes the functionalization reaction of the 5 mol % TMA polyester using acetic anhydride. The other polyester oligomers were functionalized in the same manner. The aforementioned hydroxyl-terminated (4.12 g, 2.06 mmol), TEA (0.93 g, 9.19 mmol), DMAP (0.0341 g, 0.28 mmol), and DCM (15 mL) were added to a 50 mL round-bottom flask and magnetically stirred in an oil bath. Once homogeneous, acetic anhydride (0.91 g, 8.91 mmol) in DCM (1 mL) was added to the round-bottom flask all at once. The solution was brought to a gentle reflux, where it continued stirring overnight. The light orange solution was concentrated on a rotavap and then precipitated dropwise into 75 mL of ethanol. The product was filtered, redissolved in a minimal amount of DCM, and then reprecipitated into another 75 mL of ethanol. The product was filtered, washed with methanol (3 $\times$ , 10 mL), and dried in an 80 °C vacuum oven to yield an off-white solid (3.19 g). SEC<sub>PSt</sub>  $M_n = 3.79 \times 10^3$  Da,  $\bar{D} = 2.01$  (post precipitation mass and dispersity);  $T_g = 51$  °C. <sup>1</sup>H NMR (Figure S3),  $\delta$  (ppm): 1.10–1.17 (–CH<sub>3</sub>), 2.05 (–CH<sub>3</sub>, acetyl), 3.98 (–CO–O–CH<sub>2</sub>–, end-group adjacent), 4.15–4.26 (–CO–O–CH<sub>2</sub>–), 7.75 (ArH), 8.08 (ArH), 8.17 (ArH), 8.38 (ArH).

**Acid Number Calculations.** Acid number calculations were conducted, according to ASTM D664, to monitor the progress of the polyester syntheses. In a typical experiment, approximately 1.00 g of polyester was dissolved in 50 mL of CHCl<sub>3</sub>, along with 15 drops of phenolphthalein indicator (0.1 M in MeOH). Using a burette, 0.1 M KOH in MeOH was titrated into the polyester solution with magnetic stirring. The titration was deemed complete when a light pink color had persisted for at least 30 s. The calculation that was used to determine acid number values is provided in eq 1.

$$\text{acid number} = \frac{(56.1(\text{g/mol})\text{KOH} \times \text{mL KOH in MeOH titrated} \times 0.1 \text{ M KOH in MeOH})}{(\text{g of polyester resin})} \quad (1)$$

**Thin-Film Preparation for DMA and Tensile Testing.** Several methods were attempted to prepare crosslinked thin films such as compression molding, melt casting, and deposition of the powder onto PET sheets. Unfortunately, these methods generally yielded films that contained defects such as voids or cracks. Therefore, crosslinked thin films were prepared via a solvent-casting technique to characterize the viscoelastic and tensile properties. The powder coating formulations were first dissolved in DCM (12.5 wt % solids) and then cast into aluminum trays using 3 mL of solution. Samples were immediately transferred to a 45 °C oven for 1 h. The oven temperature was then raised at 10 °C/h for the next 2 h (45 °C  $\rightarrow$  55 °C  $\rightarrow$  65 °C). Then, the oven temperature was raised at 10 °C/0.5 h for the next 1 h (65 °C  $\rightarrow$  75 °C  $\rightarrow$  85 °C). After this period, the sample was transferred to a 160 °C oven for 15–20 min to remove any residual solvent and form a uniform film. The tray was subsequently transferred to a hot plate set at 100 °C. Once the temperature equilibrated at 100 °C, the films were UV-cured for 30 s with an Omnicure S2000. A liquid light guide was used to direct the UV light, which was approximately 10 cm from the sample. The intensity of the light was maintained at 228 mW/cm<sup>2</sup>, which was confirmed by a UV-Power Puck. Rectangular samples were

Scheme 1. Two-Step Synthetic Route to the Branched, Methacrylate-Terminated Polyester Oligomers

Table 1. Characterization Summary of the Different Branched Polyester Oligomers (Not Crosslinked)<sup>a</sup>

end-group functionality	% TMA (feed)	% TMA ( <sup>1</sup> H NMR)	<i>M<sub>n</sub></i> (Da)	<i>M<sub>w</sub></i> (Da)	<i>Đ</i> ( <i>M<sub>w</sub></i> / <i>M<sub>n</sub></i> )	<i>T<sub>g</sub></i> (°C)	acid # (mg KOH/g resin)
hydroxyl	0.0	0.0	2.94 × 10 <sup>3</sup>	5.03 × 10 <sup>3</sup>	1.71	57	2.20
hydroxyl	2.5	2.8	3.85 × 10 <sup>3</sup>	7.47 × 10 <sup>3</sup>	1.94	61	3.80
hydroxyl	5.0	4.9	3.22 × 10 <sup>3</sup>	6.57 × 10 <sup>3</sup>	2.04	59	3.30
hydroxyl	7.5	7.7	3.74 × 10 <sup>3</sup>	8.64 × 10 <sup>3</sup>	2.31	62	2.40
hydroxyl	10.0	10.4	4.27 × 10 <sup>3</sup>	1.29 × 10 <sup>4</sup>	3.02	64	4.10
methacrylate	0.0	0.0	3.46 × 10 <sup>3</sup>	5.60 × 10 <sup>3</sup>	1.62	42	n.d.
methacrylate	2.5	2.7	4.47 × 10 <sup>3</sup>	8.22 × 10 <sup>3</sup>	1.84	52	n.d.
methacrylate	5.0	4.8	3.86 × 10 <sup>3</sup>	7.37 × 10 <sup>3</sup>	1.91	49	n.d.
methacrylate	7.5	7.6	4.42 × 10 <sup>3</sup>	9.72 × 10 <sup>3</sup>	2.20	47	n.d.
methacrylate	10.0	10.2	4.81 × 10 <sup>3</sup>	1.30 × 10 <sup>4</sup>	2.71	46	n.d.
acetyl	0.0	0.0	3.17 × 10 <sup>3</sup>	5.39 × 10 <sup>3</sup>	1.70	48	n.d.
acetyl	2.5	n.d.	n.d.	n.d.	n.d.	n.d.	n.d.
acetyl	5.0	5.3	3.79 × 10 <sup>3</sup>	7.62 × 10 <sup>3</sup>	2.01	51	n.d.
acetyl	7.5	n.d.	n.d.	n.d.	n.d.	n.d.	n.d.
acetyl	10.0	11.0	4.81 × 10 <sup>3</sup>	1.48 × 10 <sup>4</sup>	3.07	50	n.d.

<sup>a</sup>Where n.d. is not determined. The *T<sub>g</sub>* was determined via DSC from the 2nd heating scan using a heating rate of 20 °C/min.

prepared with a razor to the approximate dimensions of 25 × 6 × 0.20 mm<sup>3</sup> (length × width × thickness).

## RESULTS

A series of branched polyester oligomers were synthesized and characterized. The influence of branching on the rheological and thermal properties of these oligomers, before and after they were functionalized with methacrylate end groups, was evaluated. The methacrylate-functionalized oligomers were subsequently formulated with a photoinitiator package, cast as thin films, and then cured via exposure to UV light at 100 °C.

The effects that polymer architecture had on the thermal, mechanical, and viscoelastic properties of these crosslinked films was also evaluated.

**Polyester Synthesis and Characterization.** A series of branched, methacrylate-terminated polyesters were successfully synthesized via the melt polycondensation of neopentyl glycol (NPG) with terephthalic acid (TPA) and trimellitic anhydride (TMA) (Scheme 1). The extent of branching was controlled by varying the amount of TMA that was used in the feed. Hydroxyl-terminated oligomers were prepared first using a stoichiometric excess of NPG. A fixed *r*-ratio of 0.80



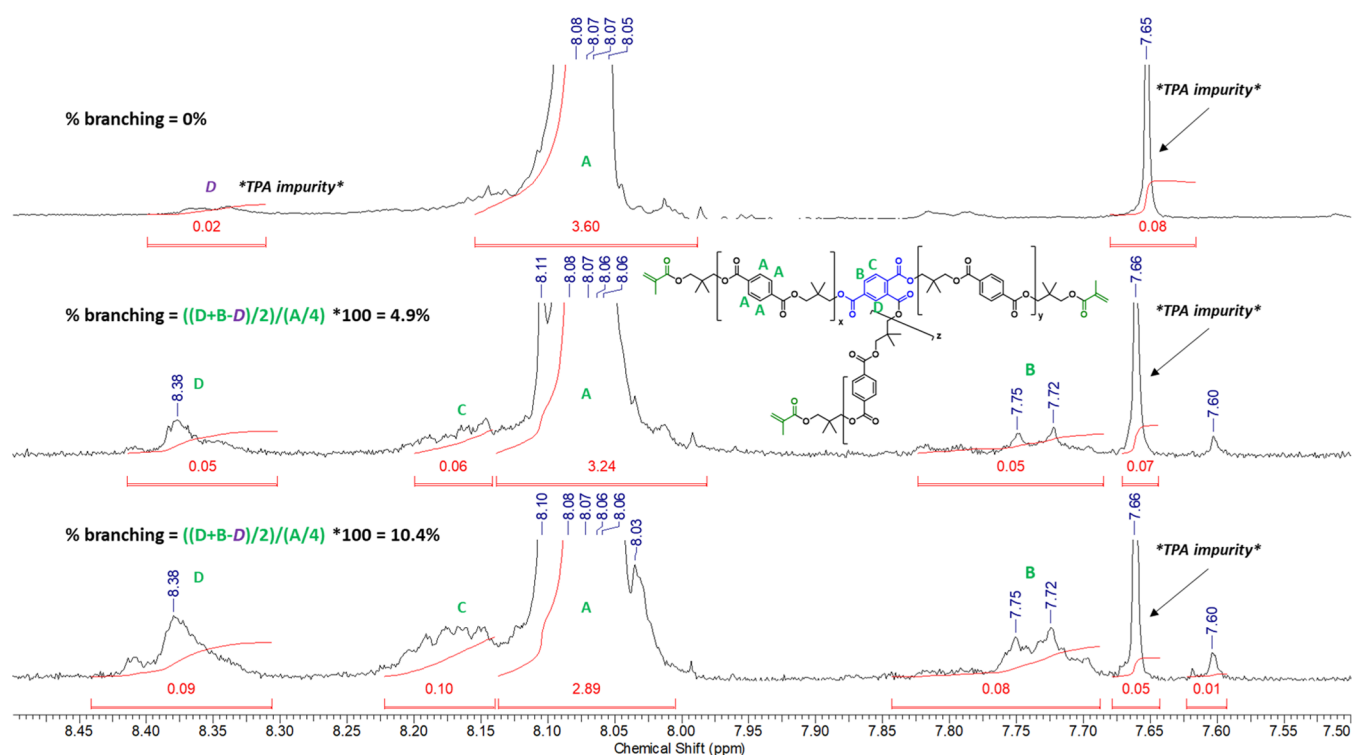


**Figure 1.**  $^1\text{H}$  NMR spectra of the 0.0, 5.0, and 10.0 mol % TMA branched polyesters displayed between 7.50 and 8.50 ppm.

(-COOH/-OH) was used to control the molecular weight and to afford oligomers with hydroxyl end groups. The hydroxyl-terminated oligomers were subsequently reacted with methacrylic anhydride (or acetic anhydride for the rheology experiments) to yield methacrylate-functional oligomers.

A total of five polyesters were prepared, having either 0.0, 2.5, 5.0, 7.5, or 10.0 mol % of TMA in the feed.  $^1\text{H}$  NMR spectroscopy was used to characterize the polyesters and to determine the amount of TMA that was incorporated into the polyester backbone (Table 1). The latter was accomplished by comparing the integration value of the aromatic TMA protons (the resonances labeled with a "B" and a "D") against the integration value of the aromatic TPA protons (the resonance labeled with an "A"). The aromatic TMA resonance labeled with a "C" was not included in the calculations because of its proximity to resonance "A". Ultimately, the TMA feed ratios matched well with the experimentally determined values. The  $^1\text{H}$  NMR spectra for the 0.0, 5.0, and 10.0 mol % TMA polyesters, displayed in the aromatic region between 7.50 and 8.50 ppm, are provided in Figure 1. The  $^1\text{H}$  NMR spectra of the hydroxyl-terminated, methacrylate-terminated, and acetyl-terminated polyesters are provided in the Supporting Information.

The molecular weight data of the various end-functionalized polyesters are provided in Table 1; the number-average molecular weight ( $M_n$ ), the weight-average molecular weight ( $M_w$ ), and the dispersity ( $M_w/M_n$ ) were determined using a linear polystyrene standard. The SEC traces of the hydroxyl-terminated and methacrylate-terminated polyesters are provided in Figures S4 and 2, respectively. Increasing the extent of branching resulted in a corresponding increase in the dispersity of the polyester. For a typical step-growth polymerization, the dispersity should be equal to 2.<sup>33</sup> However, the polyesters that contained >5 mol % TMA had dispersity values that were well above 2. This broadening of the molecular weight distribution

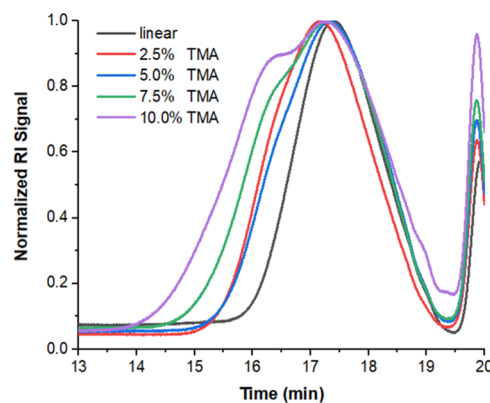


**Figure 2.** Normalized SEC traces for the methacrylate-terminated polyesters. All samples were measured against a linear polystyrene standard using THF as the eluent.

is typical for branched polymers and has been observed even when using small amounts (<1 mol %) of a branching monomer.<sup>20,34</sup> The change in the molecular weight distribution suggests that a larger concentration of both high- and low-molecular-weight species were present. High-molecular-weight shoulders were also observed for the samples that contained >5 mol % TMA, which further contributed to the increase in dispersity.

MALDI-ToF-MS was also used to characterize the 0.0 mol % TMA and 10.0 mol % TMA polyesters. The MALDI-ToF mass spectrum of the 10 mol % TMA oligomer (hydroxyl-terminated), displayed between 1975 and 2250 Da, is provided in Figure 3; additional spectra are provided in the Supporting Information (Figures S5–S7). This technique provided excellent insight into the distribution of oligomeric species that were present in both the linear and branched samples. The NPG-TPA repeat unit of 234.1 Da was identified in both

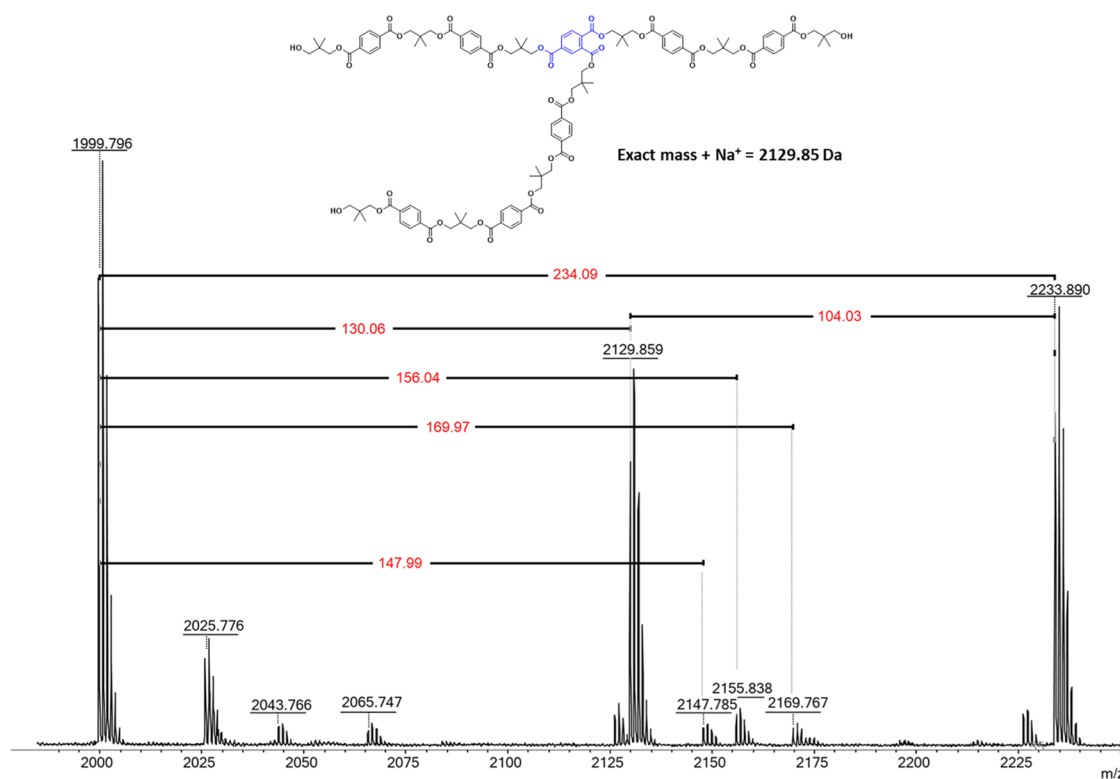


**Figure 3.** MALDI-ToF mass spectrum of the 10 mol % TMA polyester displayed between 1975 and 2250 Da.

spectra, while the NPG-TMA repeat unit of 260.23 Da was only identified in the 10.0 mol % TMA spectrum. MALDI-ToF-MS experiments also confirmed that hydroxyl groups were the predominant end group, which was in agreement with the low acid number values that were measured via acid number titrations (Table 1).

**Thermal Properties.** The thermal properties of the oligomeric resins and crosslinked polyesters are provided in Tables 1 and 2, respectively; the DSC traces are provided in

**Table 2. Thermal and Mechanical Properties of the Crosslinked Thin Films<sup>a</sup>**

% TMA (feed)	$T_g$ (°C)	$T_{d,10\%}$ (°C)	modulus (GPa)	tensile strength (MPa)	elongation at break (%)
0.0	76	425	1.2 ± 0.1	43.2 ± 4.9	5.6 ± 0.5
2.5	77	417	1.2 ± 0.1	43.8 ± 4.1	6.8 ± 1.0
5.0	76	413	1.4 ± 0.2	52.6 ± 5.4	6.9 ± 0.2
7.5	83	420	1.6 ± 0.2	51.5 ± 8.6	5.7 ± 1.4
10.0	78	419	1.4 ± 0.1	37.3 ± 1.5	4.0 ± 0.2

<sup>a</sup>The  $T_g$  was determined via DSC from the 2nd heating scan using a heating rate of 20 °C/min; the degradation temperatures were reported via TGA using a 10 °C/min heating rate.

Figure S8, while the TGA thermograms of the crosslinked polyesters are provided in Figure S9. The  $T_g$  of the oligomers was affected by the end-group functionality as well as the extent of branching. End-group effects can usually be ignored for polymeric species of sufficiently high molecular weight because the relative abundance of the ends groups is low. Accordingly, the repeat unit of the polymer dominates the thermal, rheological, and mechanical properties. However, for low-molecular-weight oligomers, end-group effects must be considered.<sup>35</sup> The hydroxyl-terminated oligomers had the

highest  $T_g$ s. This was due to the polar hydroxyl end groups that could undergo hydrogen-bonding interactions. Once the hydroxyl-terminated oligomers were functionalized, a reduction in the  $T_g$  by about 10–15 °C was observed. This abrupt decline in the  $T_g$  was due to the loss of these polar, hydrogen-bonding hydroxyl groups.<sup>36</sup> The extent of branching also affected the  $T_g$  of the oligomer. Increasing the extent of branching led to an increase in the  $T_g$  of the hydroxyl-terminated oligomers. This was due to the increase in the functionality of the resin, which afforded more hydroxyl end groups that could participate in hydrogen-bonding interactions. However, once these oligomers were functionalized with acetyl or methacrylate end groups, the opposite trend was observed. This was due to the increase in the free volume of the material. After the methacrylated oligomers were cross-linked upon exposure to UV light, a large increase in the  $T_g$  by about 20–30 °C was observed. All crosslinked samples had excellent thermal stabilities with 5% degradation temperatures ( $T_{d,5\%}$ ) that were well above 300 °C. Introduction of TMA appeared to have no effect on the thermal stability of the crosslinked films.

**Zero-Shear Melt Viscosity.** The rheological properties of branched polymers can be significantly different from linear polymers of similar chemical composition. In general, branched polymers will display a lower zero-shear melt viscosity than linear polymers of the same molecular weight. This is due to a lack of chain entanglements in branched polymers, a consequence of their globular structure and smaller hydrodynamic volume. However, the opposite trend has also been observed.<sup>34,37,38</sup> When the latter scenario is encountered, the branched polymers typically have broad molecular weight distributions or have branches with molecular weights that are well above the molecular weight of entanglement ( $M_e$ ). Nonetheless, it is important to understand how changes to

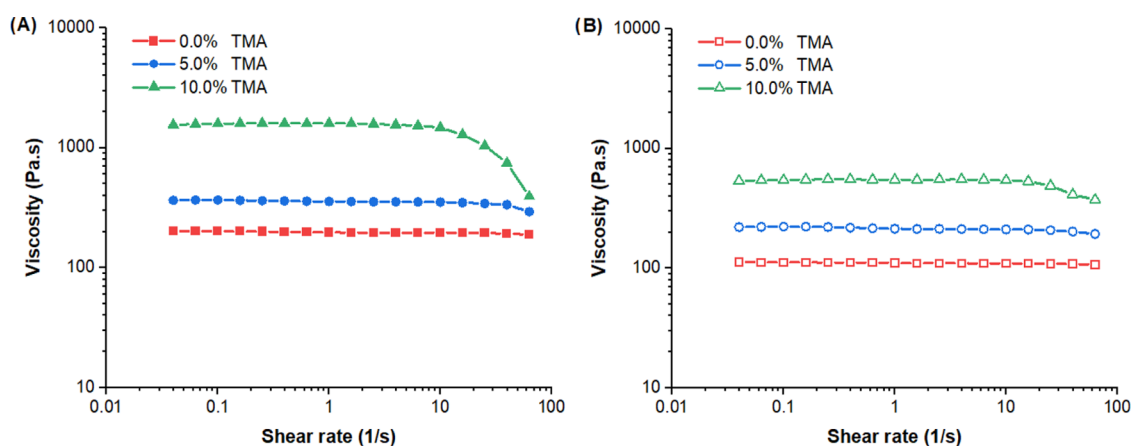


**Figure 4.** Zero-shear viscosity measurements as a function of shear rate for the (A) hydroxyl-terminated oligomers (closed figures) and for the (B) acetyl-terminated oligomers (open figures).

**Table 3.** Viscoelastic Properties of the Crosslinked Polyester Films

% TMA (feed)	$E'$ @ 25 °C (GPa)	$E'_{\min}$ @ $T_g + 50$ °C (MPa)	tan delta max (°C)	tan delta breadth at 1/2 height (°C)	$M_c$ (g/mol)
0.0	$2.0 \pm 1.0$	$4.6 \pm 0.7$	$100 \pm 3$	$20 \pm 1$	$2,800 \pm 470$
2.5	$1.9 \pm 1.2$	$5.2 \pm 1.1$	$96 \pm 0$	$23 \pm 4$	$2,400 \pm 560$
5.0	$2.1 \pm 1.2$	$7.9 \pm 0.6$	$102 \pm 4$	$20 \pm 2$	$1,600 \pm 130$
7.5	$2.2 \pm 0.4$	$10.8 \pm 0.4$	$105 \pm 2$	$18 \pm 1$	$1,200 \pm 40$
10.0	$2.2 \pm 0.8$	$9.8 \pm 0.2$	$110 \pm 2$	$19 \pm 1$	$1,300 \pm 20$

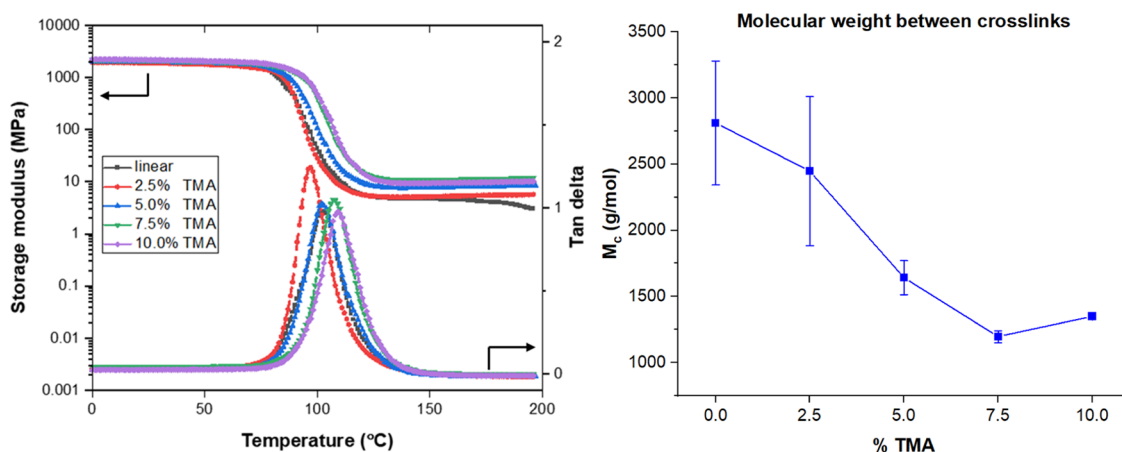


**Figure 5.** Dynamic mechanical analysis of the crosslinked polyester films (left) and  $M_c$  vs TMA loading level relationship (right). Samples were analyzed in tension mode, with a strain rate of 0.1%, a frequency of 1 Hz, and a heating rate of 4 °C/min.

the architecture of a polymer will affect its rheological properties.

Rheology experiments were conducted on the branched polyester oligomers to understand how end-group functionality and the extent of branching affected the zero-shear melt viscosity. All samples were analyzed at a fixed temperature of  $T_g + 50$  °C. Figure 4 illustrates the zero-shear melt viscosity of the samples before and after they were functionalized with acetyl groups. Increasing the extent of branching led to an exponential increase in the zero-shear melt viscosity of the sample (Figure S9). It is suspected that the higher zero-shear melt viscosities of the branched samples were due to the broader molecular weight distributions. This behavior was observed for both the hydroxyl-terminated oligomers and the acetyl-terminated oligomers. However, the hydroxyl-terminated samples had higher viscosities than the acetyl-terminated analogues. This was a consequence of the hydroxyl end groups

participating in intermolecular hydrogen-bonding interactions with one another.<sup>39</sup> When the sample was functionalized with acetyl groups, a decrease in the zero-shear melt viscosity occurred. The critical shear rate, which is the shear rate where shear thinning begins to occur, was also affected by branching. When the extent of branching increased, the critical shear rate decreased. For example, the linear oligomer did not exhibit a critical shear rate in the shear rate range that was used. However, the 10 mol % TMA oligomer exhibited a critical shear rate of  $16 \text{ s}^{-1}$ .

**Viscoelastic and Tensile Properties.** Young's modulus, ultimate tensile strength, and % elongation at break were characterized via tensile tests at room temperature; the results are summarized in Table 2. All samples exhibited brittle failure due to the rigid nature of thermoset polyester powder coatings. In general, Young's modulus increased with the degree of branching, spanning a range of  $\sim 1.2$  to 1.6 GPa. This increase

in the Young's modulus was the result of the higher crosslink density in the more branched samples. The opposite trend was observed for the % elongation at break, i.e., increasing the extent of branching led to a decrease in the % elongation at break. This trend was also attributed to the higher crosslink density of the more branched samples. The 2.5% TMA sample was an outlier for this general trend, but it is suspected that this was due to the pre-polymer having a higher MW before crosslinking (see SEC data). Consequently, the higher molecular weight of the pre-polymer reduced the sample's crosslink density and increased its elastic character.

Dynamic mechanical analysis (DMA) experiments highlighted the viscoelastic behavior of the crosslinked films and is presented in Table 3 and Figure 5. All of the crosslinked samples displayed similar storage modulus values of  $\sim 2$  GPa in the glassy regime; these results were similar to a thermally cured polyester powder coating.<sup>40</sup> At the onset of the  $T_g$ , a precipitous decline in the storage modulus occurred. Noticeable differences were observed for the storage modulus in the rubbery plateau ( $E'_{\min}$ ). Higher degrees of branching increased the  $E'_{\min}$ , indicative of a more densely crosslinked polymer network. For example, the linear polyester (0 mol % TMA) had an  $E'_{\min}$  of  $4.6 \pm 0.7$  MPa, while the 5.0 mol % TMA crosslinked polyester had an  $E'_{\min}$  of  $7.9 \pm 0.6$  MPa. This corresponded to a difference in the molecular weight between crosslinks by  $\sim 1200$  g/mol (Table 3 and Figure 5). The  $\alpha$ -relaxation in the tan delta curve also shifted to higher temperatures with an increase in the degree of branching, indicative of higher  $T_g$ s, which is typical for more highly crosslinked materials. However, no significant changes in the height of the  $\alpha$ -relaxation or its breadth at half height were observed, suggesting that homogeneously crosslinked networks were obtained. The molecular weight between crosslinks ( $M_c$ ), which is presented in Table 3, was calculated using eqs 2 and 3 (where  $\nu$  is the crosslink density).

$$\nu = \frac{E'_{\min}}{(3^* RT)} \quad (2)$$

$$M_c = \frac{\rho}{\nu} \quad (3)$$

**Gel Content.** Soxhlet extractions were conducted to measure the gel content of the crosslinked films (Figure 6). The lightly branched samples (0.0 and 2.5 mol % TMA) had relatively low gel contents ( $\sim 90\%$ ), suggesting that these films contained unreacted oligomers and photoinitiator molecules. Conversely, the samples that contained 5.0, 7.5, and 10.0 mol % TMA were almost completely insoluble, with gel contents that exceeded 97%. The higher gel contents suggested that films with higher crosslink densities were obtained, in agreement with the results obtained by DMA. Additionally, the higher gel contents also suggest that there was a higher degree of unsaturated double bond conversion.<sup>41</sup>

## DISCUSSION

Several studies have explored the use of hyperbranched or dendritic polymers for UV-curable powder coating applications.<sup>29,31,32,42,43</sup> Unfortunately, most of these systems are impractical for commercial applications because they are too expensive or because they exhibit even worse properties than conventional systems. Until now, there have been no systematic studies that have investigated how the extent of branching affects the properties of conventional UV-curable

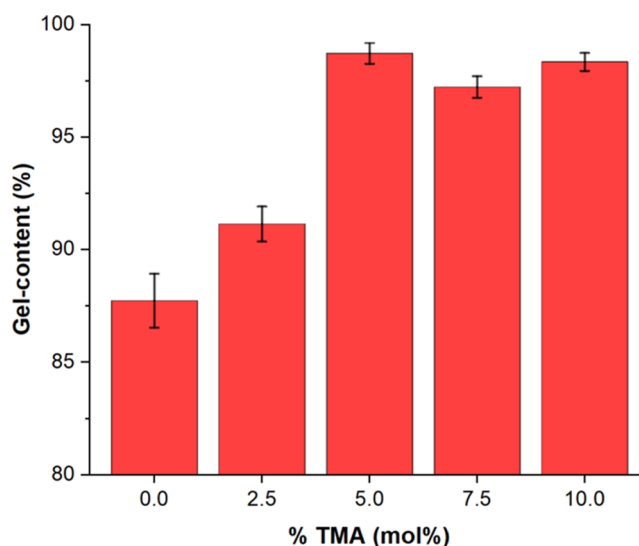


**Figure 6.** Gel content of the various branched crosslinked films after 24 h of Soxhlet extraction with THF.

polyester powder coatings (i.e., those that are principally derived from NPG and TPA). A thorough understanding of how the extent of branching affects the properties of these resins, both before and after curing, is essential for optimizing the performance of these coating systems.

In this study, a series of branched polyesters were prepared with variable degrees of branching. The degree of branching was controlled by changing the amount of TMA that was incorporated into the feed. A stoichiometric excess of diol (1.00:0.80 -OH/-COOH) was used to control the molecular weight of the polyester and yielded oligomers with hydroxyl end groups. A fixed  $r$ -ratio of 0.80 was used for all samples to prevent them from crosslinking prematurely. The Flory–Stockmayer theory was applied to determine  $r$ -ratios that would, in theory, afford gel-free products. Accordingly, the polyesters were designed so that the critical extent of conversion ( $p_c$ ) was well above 1. Table 4 below provides

**Table 4.** The Critical Extents of Conversion ( $p_c$ ) for the Different Branched Polyesters with  $r$ -Ratios of Either 0.75, 0.80, 0.85, or 0.90

polyester	$r$ -ratio			
	0.75 ( $p_c$ )	0.80 ( $p_c$ )	0.85 ( $p_c$ )	0.90 ( $p_c$ )
0.0% TMA	1.155	1.118	1.085	1.054
2.5% TMA	1.132	1.098	1.066	1.037
5.0% TMA	1.112	1.079	1.049	1.021
7.5% TMA	1.093	1.062	1.033	1.007
10.0% TMA	1.076	1.046	1.018	0.993

the  $p_c$  values for the polyesters if they were prepared with  $r$ -ratios of either 0.75, 0.80, 0.85, or 0.90. The calculations suggested that only the 10 mol % TMA polyester with a stoichiometric equivalency of 0.90 would have resulted in a gelled polymer network. As such, a series of polyester oligomers with an  $r$ -ratio of 0.85 were prepared first. However, even at this stoichiometric ratio, some insoluble material was obtained from the branched polyester samples that contained 7.5 and 10.0 mol % TMA; only the 0, 2.5, and 5.0 mol % samples were completely soluble in common organic solvents such as THF, DCM, or  $\text{CHCl}_3$ . When an  $r$ -ratio of 0.80 was



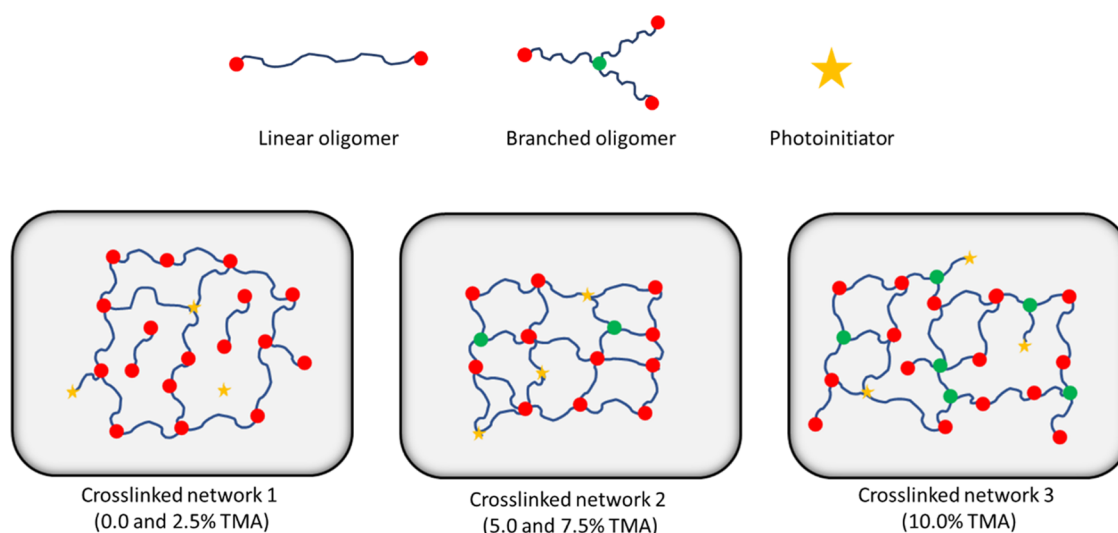


**Figure 7.** Schematic illustration depicting the three different types of crosslinked networks that were encountered in this study. Network (1) is representative of the linear (0 mol % TMA) and 2.5 mol % TMA samples, where unreacted oligomers and photoinitiator molecules are present in the network, in addition to dangling chain ends; network (2) is representative of the 5.0 mol % TMA and 7.5 mol % TMA samples, where the most uniform, densely crosslinked networks were encountered with a negligible amount of unreacted species; and network (3) is representative of the 10.0 mol % TMA sample, where the extent of branching is so great that the crosslinked network vitrifies before the system completely reacts, leaving dangling chain ends in the network. However, network 3 differs from network 1 in that network 1 contains significantly more unreacted oligomers and/or photoinitiator molecules.

employed, all of the branched polyesters were completely soluble in the aforementioned solvents. The  $p_c$  value was determined from eqs 4 and 5 below.

$$\rho = \frac{N_C f_C}{N_A f_A + N_C f_C} \quad (4)$$

$$p_c = 1/\sqrt{1 + \rho(f - 2)} \quad (5)$$

where  $N_C$  is the number of moles of the polyfunctional monomer;  $N_A$  is the number of moles of the monomer with the same functionality as the polyfunctional monomer;  $f_C$  is the functionality of the polyfunctional monomer;  $f_A$  is the functionality of the difunctional monomer, A; and  $f$  is the functionality of the polyfunctional monomer, respectively.

Powder coating resins frequently employ a small amount of a branching monomer such as trimethylolpropane (TMP) or trimellitic anhydride (TMA) to increase the functionality of the oligomer and to ensure that it remains an amorphous solid. However, the introduction of branching monomers into the backbone of a polymer is also an excellent way to alter its rheological properties. The zero-shear melt viscosity of a powder coating resin is especially important because of its relationship with film formation. Lower zero-shear melt viscosities exhibit better leveling and flow properties, thereby affording smoother films.<sup>29</sup> In this study, the linear and lightly branched resins ( $\leq 5.0$  mol % TMA) had lower zero-shear melt viscosities than the highly branched (7.5 and 10.0 mol % TMA) resins. This suggests that smoother films, free of orange peel defects, would be obtained from the former. However, the strong shear-thinning behavior exhibited by the more highly branched systems is advantageous from a processing perspective. When these resins are ultimately formulated into powder coatings via extrusion, the lower melt viscosities displayed at high shear rates will increase throughput for industrial-scale production. As such, a careful balance of the extent of branching should be used to provide a resin system

with good processability and a low-enough zero-shear melt viscosity to afford good leveling and film formation.

DMA experiments were also conducted to highlight the viscoelastic properties of the crosslinked films over the temperature range of 0–200 °C. Increasing the extent of branching led to a corresponding increase in the  $\alpha$ -relaxation and the  $E'_{\min}$ . However, there were no changes in the breadth of the  $\alpha$ -relaxation in the tan delta curve. The breadth of the  $\alpha$ -relaxation is closely related to the heterogeneity of a polymer network.<sup>44</sup> Previous studies have shown that polyfunctional crosslinkers and highly branched systems tend to afford more heterogeneous networks due to the formation of microgels and phase separation.<sup>45–48</sup> These densely crosslinked regions are undesirable because they can act as defect sites that negatively impact the mechanical properties of the film. Here, no significant changes were observed in the height or the breadth of the  $\alpha$ -relaxation, suggesting that homogeneous crosslinked networks were obtained, regardless of the extent of branching.

The concert of DMA, DSC, tensile, and Soxhlet extraction experiments provided insight into the crosslinked network structures of the different branched polyesters. DMA experiments demonstrated that all crosslinked networks were homogeneous, as evidenced by the tan delta behavior. However, analysis of the  $E'_{\min}$  shows that different crosslinked microstructures must be present. In theory, the 10 mol % TMA sample should have the highest crosslink density since the molecular weight between crosslinks would be the lowest.<sup>47,49</sup> However, the crosslink density for this sample actually decreased relative to the 7.5 mol % TMA sample. DSC also showed that the  $T_g$  of the 10 mol % TMA polyester was less than the 7.5 mol % TMA sample, which suggested a lower crosslink density because of the relationship between crosslink density and  $T_g$ . Tensile tests identified a lower modulus for the 10 mol % sample and also lower tensile strengths, again suggesting that this sample had a lower crosslink density than the 7.5 mol % TMA sample. Finally, Soxhlet extraction experiments showed that the samples containing  $\geq 5.0$  mol %

TMA were almost completely crosslinked with gel contents that were  $\geq 97\%$ . Based on these results, it is hypothesized that three types of crosslinked network scenarios were encountered: (1) the networks created by the 0 mol % TMA and 2.5 mol % TMA polyesters, which contained unreacted oligomers and photoinitiator molecules trapped within the vitrified network; (2) the networks created by the 5.0 mol % TMA and 7.5 mol % TMA samples, which had the most thorough and complete crosslinked network structures; and (3) the network created by the 10 mol % TMA, which was highly crosslinked but had dangling chain ends that plasticize the network and reduce its crosslink density. Figure 7 illustrates the different crosslinked network structures that were encountered in this study.

## CONCLUSIONS

A series of branched, UV-curable polyester oligomers containing methacrylate end groups were synthesized and characterized. The thermal properties were affected by the functionality of the end group as well as the extent of branching. The hydroxyl-terminated oligomers had  $T_g$ s that were 10–15 °C higher than the methacrylate-terminated analogues due to the hydrogen-bonding interactions of the hydroxyl groups. Increasing the extent of branching increased the  $T_g$  of the hydroxyl-terminated oligomers, whereas the opposite trend was observed for the methacrylate-terminated oligomers. Rheology experiments showed that the zero-shear melt viscosity increased with the extent of branching, a consequence of the molecular weight distribution for these oligomers. DMA experiments probed the viscoelastic properties of the crosslinked thin films and found that the  $\alpha$ -relaxation temperature and the  $E'_{\min}$  increased with the extent of branching. DMA also showed that all crosslinked networks were homogeneously crosslinked, with no signs of phase separation or microgel formation, regardless of the extent of branching. The concert of DMA, DSC, tensile testing, and Soxhlet extraction experiments confirmed that different crosslinked networks were encountered. Linear and lightly branched samples (0.0 and 2.5 mol % TMA) yielded networks with unreacted material, while too much branching (10.0 mol % TMA) yielded networks with dangling chain ends. The most efficiently crosslinked networks, which were obtained from the moderately branched oligomers (5.0 and 7.5 mol % TMA), had superior film properties (i.e., crosslink density, tensile strength, % elongation at break, etc.). Ultimately, the insights derived from this study highlight the importance of using controlled amounts of branching when optimizing the performance of UV-curable polyester powder coating resins.

## ASSOCIATED CONTENT

### Supporting Information

The Supporting Information is available free of charge at <https://pubs.acs.org/doi/10.1021/acs.iecr.2c00697>.

Additional figures, including  $^1\text{H}$  NMR spectra, GPC traces, DSC and TGA thermograms, and MALDI-ToF spectra, and zero-shear viscosity vs % TMA relationship (PDF)

## AUTHOR INFORMATION

### Corresponding Author

Mark D. Soucek — School of Polymer Science and Polymer Engineering, University of Akron, Akron, Ohio 44325, United

States; [orcid.org/0000-0003-3865-4504](https://orcid.org/0000-0003-3865-4504);

Email: [msoucek@uakron.edu](mailto:msoucek@uakron.edu)

## Authors

Theodore J. Hammer — School of Polymer Science and Polymer Engineering, University of Akron, Akron, Ohio 44325, United States

Coleen Pugh — School of Polymer Science and Polymer Engineering, University of Akron, Akron, Ohio 44325, United States; Department of Chemistry and Biochemistry, Wichita State University, Wichita, Kansas 67260, United States; [orcid.org/0000-0002-1476-0890](https://orcid.org/0000-0002-1476-0890)

Complete contact information is available at: <https://pubs.acs.org/10.1021/acs.iecr.2c00697>

## Author Contributions

The manuscript was written through contributions of all authors. All authors have given approval to the final version of the manuscript.

## Notes

The authors declare no competing financial interest.

## ACKNOWLEDGMENTS

This research was funded by The University of Akron's School of Polymer Science and Polymer Engineering.

## REFERENCES

- (1) Jones, F. N.; Nichols, M. E.; Pappas, S. P. Powder Coatings. *Org. Coat. Sci. Technol.* **2017**, 385–402.
- (2) McGinniss, V. Ultraviolet Curable Epoxy-Polyester Powder Paints. U.S. Patent US4,129,488 1976.
- (3) Udding-louwrier, S.; Baijards, R. A.; Jong, E. S. New Developments in Radiation-Curable Powder Coatings. *J. Coat. Technol.* **2000**, 72, 71–75.
- (4) Buysens, K.; Maetens, D.; Hammerton, D. Performance Optimization of UV Powder Coatings by Combining Resin Systems; RadTech Europe, 2004.
- (5) Moens, L.; Loutz, J.-M.; Maetens, D.; Loosen, P.; Van Kerckhove, M. Powder Composition of Crystalline Polyesters Containing End Methacrylyl Groups. U.S. Patent US5,639,560 1996.
- (6) Moens, L.; Loutz, J.-M.; Maetens, D.; Loosen, P.; Van Kerckhove, M. Powder Compositions with Semicrystalline Polyester and Amorphous Polyester Base Containing Terminal Methacryloyl Groups. U.S. Patent US6,380,279 B1 1997.
- (7) Twilight, F.; Van Der Linde, R. Radiation Curable Binder Composition for Powder Paint Formulations. U.S. Patent US5,703,198 1997.
- (8) Gao, C.; Yan, D. Hyperbranched Polymers: From Synthesis to Applications. *Prog. Polym. Sci.* **2004**, 29, 183–275.
- (9) McKee, M. G.; Unal, S.; Wilkes, G. L.; Long, T. E. Branched Polyesters: Recent Advances in Synthesis and Performance. *Prog. Polym. Sci.* **2005**, 30, 507–539.
- (10) Matyjaszewski, K.; Tsarevsky, N. V. Nanostructured Functional Materials Prepared by Atom Transfer Radical Polymerization. *Nat. Chem.* **2009**, 1, 276–288.
- (11) Claesson, H.; Scheurer, C.; Malmström, E.; Johansson, M.; Hult, A.; Paulus, W.; Schwalm, R. Semi-Crystalline Thermoset Resins: Tailoring Rheological Properties in Melt Using Comb Structures with Crystalline Grafts. *Prog. Org. Coatings* **2004**, 49, 13–22.
- (12) Pesetskii, S. S.; Jurkowski, B.; Olkhov, Y. A.; Olkhova, O. M.; Storozhuk, I. P.; Mozheiko, U. M. Molecular and Topological Structures in Polyester Block Copolymers. *Eur. Polym. J.* **2001**, 37, 2187–2199.
- (13) Zhang, M.; Moore, R. B.; Long, T. E. Melt Transesterification and Characterization of Segmented Block Copolyesters Containing

- 2,2,4,4-Tetramethyl-1,3-Cyclobutanediol. *J. Polym. Sci., Part A: Polym. Chem.* **2012**, *50*, 3710–3718.
- (14) Kang, H.; Lin, Q.; Armentrout, R. S.; Long, T. E. Synthesis and Characterization of Telechelic Poly(Ethylene Terephthalate) Sodio-sulfonate Ionomers. *Macromolecules* **2002**, *35*, 8738–8744.
- (15) Lo Verso, F.; Likos, C. N. End-Functionalized Polymers: Versatile Building Blocks for Soft Materials. *Polymer* **2008**, *49*, 1425–1434.
- (16) Eriksson, M.; Hult, K.; Malmström, E.; Johansson, M.; Trey, M.; Martinelle, M. One-Pot Enzymatic Polycondensation to Telechelic Methacrylate-Functional Oligoesters Used for Film Formation. *Polym. Chem.* **2011**, *2*, 714–719.
- (17) Jayakannan, M.; Ramakrishnan, S. Synthesis and Thermal Analysis of Branched and “Kinked” Poly (Ethylene Terephthalate). *J. Polym. Sci., Part A: Polym. Chem.* **1998**, *36*, 309–317.
- (18) Manaresi, P.; Munari, A.; Pilati, F.; Alfonso, G. C.; Russo, S.; Sartirana, M. L. Synthesis and Characterization of Branched Poly(Ethylene Terephthalate). *Polymer* **1986**, *27*, 955–960.
- (19) Malmström, E.; Johansson, M.; Hult, A. Hyperbranched Aliphatic Polyesters. *Macromolecules* **1995**, *28*, 1698–1703.
- (20) Unal, S.; Ozturk, G.; Sisson, K.; Long, T. E. Poly-(Caprolactone) Containing Highly Branched Segmented Poly(Ester Urethane)s via A2 with Oligomeric B3 Polymerization. *J. Polym. Sci., Part A: Polym. Chem.* **2008**, *46*, 6285–6295.
- (21) Zhang, Y.; Asif, A.; Shi, W. Highly Branched Polyurethane Acrylates and Their Waterborne UV Curing Coating. *Prog. Org. Coatings* **2011**, *71*, 295–301.
- (22) Hawker, C. J.; Lee, R.; Fréchet, J. M. J. One-Step Synthesis of Hyperbranched Dendritic Polyesters. *J. Am. Chem. Soc.* **1991**, *113*, 4583–4588.
- (23) Wooley, K. L.; Hawker, C. J.; Pochan, J. M.; Fréchet, J. M. J. Physical Properties of Dendritic Macromolecules: A Study of Glass Transition Temperature. *Macromolecules* **1993**, *26*, 1514–1519.
- (24) Shi, W.; Rånby, B. Photopolymerization of Dendritic Methacrylated Polyesters. I. Synthesis and Properties. *J. Appl. Polym. Sci.* **1996**, *59*, 1937–1944.
- (25) Shi, W.; Rånby, B. Photopolymerization of Dendritic Methacrylated Polyesters. II. Characteristics and Kinetics. *J. Appl. Polym. Sci.* **1996**, *59*, 1945–1950.
- (26) Jones, F. N.; Nichols, M. E.; Pappas, S. P. Polyester Resins. *Org. Coat. Sci. Technol.* **2017**, 141–150.
- (27) Yu, J.; Lin, F.; Becker, M. L. Branched Amino Acid Based Poly(Ester Urea)s with Tunable Thermal and Water Uptake Properties. *Macromolecules* **2015**, *48*, 2916–2924.
- (28) Johansson, M.; Malmström, E.; Hult, A.; Jansson, A. Novel Concept for Low Temperature Curing Powder Coatings Based on Hyperbranched Polyesters. *J. Coatings Technol.* **2000**, *72*, 49–54.
- (29) Johansson, M.; Hult, A.; Claesson, H.; Malmström, E. Synthesis and Characterisation of Star Branched Polyesters with Dendritic Cores and the Effect of Structural Variations on Zero Shear Rate Viscosity. *Polymer* **2002**, *43*, 3511–3518.
- (30) Claesson, H.; Malmström, E.; Johansson, M.; Hult, A.; Doyle, M.; Manson, J. E. Rheological Behaviour during UV-Curing of a Star-Branched Polyester. *Prog. Org. Coatings* **2002**, *44*, 63–67.
- (31) Wei, H.; Liang, H.; Zou, J.; Shi, W. UV-Curable Powder Coatings Based on Dendritic Poly(Ether-Amide). *J. Appl. Polym. Sci.* **2003**, *90*, 287–291.
- (32) Cheng, X.-e.; Huang, Z.; Liu, J.; Shi, W. Synthesis and Properties of Semi-Crystalline Hyperbranched Poly(Ester-Amide) Grafted with Long Alkyl Chains Used for UV-Curable Powder Coatings. *Prog. Org. Coatings* **2007**, *59*, 284–290.
- (33) Odian, G. Step Polymerization. In *Principles of Polymerization*, 2004; pp 39–197.
- (34) Yoon, K. H.; Min, B. G.; Park, O. O. Effect of Multifunctional Comonomers on the Properties of Poly(Ethylene Terephthalate) Copolymers. *Polym. Int.* **2002**, *51*, 134–139.
- (35) Danusso, F.; Levi, M.; Gianotti, G.; Turri, S. End Unit Effect on the Glass Transition Temperature of Low-Molecular-Weight Polymers and Copolymers. *Polymer* **1993**, *34*, 3687–3693.
- (36) Khalyavina, A.; Häußler, L.; Lederer, A. Effect of the Degree of Branching on the Glass Transition Temperature of Polyesters. *Polymer* **2012**, *53*, 1049–1053.
- (37) Berry, G. C.; Hobbs, L. M.; Long, V. C. Solution and Bulk Properties of Branched Polyvinyl Acetates Part IV - Melt Viscosity. *Polymer* **1964**, *5*, 31–50.
- (38) Wood-Adams, P. M.; Dealy, J. M.; DeGroot, A. W.; Redwine, O. D. Effect of Molecular Structure on the Linear Viscoelastic Behavior of Polyethylene. *Macromolecules* **2000**, *33*, 7489–7499.
- (39) Liu, Q.; Jain, T.; Peng, C.; Peng, F.; Narayanan, A.; Joy, A. Introduction of Hydrogen Bonds Improves the Shape Fidelity of Viscoelastic 3D Printed Scaffolds While Maintaining Their Low-Temperature Printability. *Macromolecules* **2020**, *53*, 3690–3699.
- (40) Ståhlberg, D.; Johansson, M. Properties of Powder Coatings in Load Carrying Construction. *J. Coatings Technol. Res.* **2005**, *2*, 473–481.
- (41) Yu, Q.; Nauman, S.; Santerre, J. P.; Zhu, S. Photopolymerization Behavior of Di(Meth)Acrylate Oligomers. *J. Mater. Sci.* **2001**, *36*, 3599–3605.
- (42) Johansson, M.; Malmström, E.; Jansson, A.; Hult, A. Novel Concept for Low Temperature Curing Powder Coatings Based on Hyperbranched Polyesters. *J. Coatings Technol.* **2000**, *72*, 49–54.
- (43) Löwenhielm, P.; Nyström, D.; Johansson, M.; Hult, A. Aliphatic Polycarbonate Resins for Radiation Curable Powder Coatings. *Prog. Org. Coatings* **2005**, *54*, 269–275.
- (44) Simon, G. P.; Allen, P. E. M.; Williams, D. R. G. Properties of Dimethacrylate Copolymers of Varying Crosslink Density. *Polymer* **1991**, *32*, 2577–2587.
- (45) Nebioglu, A.; Soucek, M. D. Reaction Kinetics and Microgel Particle Size Characterization of Ultraviolet-Curing Unsaturated Polyester Acrylates. *J. Polym. Sci., Part A: Polym. Chem.* **2006**, *44*, 6544–6557.
- (46) Nebioglu, A.; Soucek, M. D. Microgel Formation and Thermo-Mechanical Properties of UV-Curing Unsaturated Polyester Acrylates. *J. Appl. Polym. Sci.* **2008**, *107*, 2364–2374.
- (47) Young, J. S.; Kannurpatti, A. R.; Bowman, C. N. Effect of Comonomer Concentration and Functionality on Photopolymerization Rates, Mechanical Properties and Heterogeneity of the Polymer. *Macromol. Chem. Phys.* **1998**, *199*, 1043–1049.
- (48) Ortega, A. M.; Kasprzak, S. E.; Yakacki, C. M.; Diani, J.; Greenberg, A. R.; Gall, K. Structure – Property Relationships in Photopolymerizable Polymer Networks: Effect of Composition on the Crosslinked Structure and Resulting Thermomechanical Properties of a (Meth) Acrylate-Based System. *J. Appl. Polym. Sci.* **2008**, *110*, 1559–1572.
- (49) Elliott, J. E.; Bowman, C. N. Predicting Network Formation of Free Radical Polymerization of Multifunctional Monomers. *Polym. React. Eng.* **2002**, *10*, 1–19.